Proc. of the 9th Intl. Conf. of Asian Society for Precision Engg. and Nanotechnology (ASPEN 2022)
15–18 November 2022, Singapore. Edited by Nai Mui Ling Sharon and A. Senthil Kumar
doi://10.3850/978-981-18-6021-8_OR-01-0107

Influence of TiC Reinforcement Particles on the Mechanical Properties and Microstructures of Heat-Treated IN718 Composite

Duy Nghia Luu[1], Sharon Mui Ling Nai[1,#], Wei Zhou[2,#]

1 Singapore Institute of Manufacturing Technology, Agency for Science, Technology and Research (A*STAR), 73 Nanyang Drive, Singapore 637662, Singapore
2 School of Mechanical and Aerospace Engineering, Nanyang Technological University, 50 Nanyang Avenue, Singapore 639798, Singapore
Corresponding Author / Email: mlnai@simtech.a-star.edu.sg (Sharon Mui Ling Nai)
mwzhou@ntu.edu.sg or wzhou@cantab.net (Wei Zhou)

KEYWORDS: Selective laser melting, Additive manufacturing, Inconel 718, TiC, Mechanical properties, Microstructures

In this study, TiC reinforcement particles were used to fabricate IN718/TiC composite using selective laser melting technology. The interactions between the reinforcement particles and the IN718 matrix during the solutionizing and aging processes were investigated. It was found that the addition of TiC particles contributed to the reduction of solute segregation at the grain boundary and the susceptibility to hot cracking. The results indicated that the solute materials (Nb and Mo) were absorbed by TiC particles through Ostwald ripening mechanism instead of diffusing to the grain boundaries. In addition, noticeable improvements in strength and microhardness were observed after heat treatment in comparison with the as-printed sample. It was shown that the addition of TiC particles also facilitated the formation of nano-sized carbonitride precipitates in the as-printed sample. These precipitates could still be observed after the heat treatment process and contributed significantly to the grain refinement and strengthening of the heat-treated samples. Moreover, the combination of finer grains and segregation mitigation resulted in γ′ and γ″ precipitates being distributed more homogeneously. This study has demonstrated the significant benefits of TiC particles in further improving the mechanical performance of selective laser melted IN718.

NOMENCLATURE

AP-0 = As printed IN718 without reinforcement
AP-1 = As printed IN718 with 1 wt.% TiC reinforcement
X-0 or X-1 where X is a number indicates the solutionizing temperature for sample AP-0 or AP-1, respectively.
XA-0 or XA-1 = aged X-0 and X-1, respectively.

1. Introduction

IN718 possesses excellent weldability due to its sluggish response of precipitation hardening [1], making it very suitable to fabricate IN718 MMCs by AM. Apart from understanding the strengthening mechanisms between the reinforcement particles and the metal matrix which include grain strengthening, Orowan strengthening, work hardening, etc., [2] it is also necessary to understand the interactions between the reinforcement and the precipitates in the IN718 matrix during this process. The material must undergo proper thermal treatment which often consists of solutionizing and aging treatment. As a result, hardness and tensile strength are improved due to the increase in γ′ and γ″ precipitation and growth [3]. Even though other pieces of literature that study the same material system [4]–[6] have reported the influence of TiC on the mechanical properties of heat-treated IN718, they did not solutionize beyond 1100 ^{o}C. Moreover, the effects of TiC addition on segregation behavior in the IN718 matrix are not reported.

2. Microstructural characterization

2.1 As-printed samples

Using the optimized parameters, the as-printed samples are fully dense, and the micron-TiC particles are seen to be evenly distributed within the matrix. SEM analysis was carried out on etched samples as shown in Fig. 1. The vertical, light color stripes are identified using EDX analysis to be Laves phase which has high concentrations of Nb and Mo [7]. Nano-sized precipitates are also observed in the matrix and are identified to be carbonitride precipitates that are rich in Ti, Nb, N, and C. The number of precipitates is much higher in sample AP-1. The formation of these nano-sized precipitates is facilitated by the

micron-TiC addition, which can be attributed to the partial dissolution of micron-TiC particles that introduced additional Ti and C into the matrix [8].

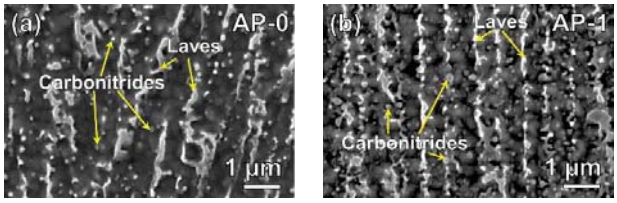

Fig. 1 SEM images of samples AP-0 (a) and AP-1 (b).

2.2 Solutionized samples

The presence of carbonitride precipitates is confirmed after solutionization as seen in Fig. 2. A higher number of precipitates is also observed in the reinforced sample. The δ phase starts to form as small needle-like precipitates in both samples 1075-0 and 1075-1. Laves phase no longer exists as small precipitates arranged in several straight lines, but as large, blocky precipitates instead. The carbonitride precipitates did not only exist as individual ones but also formed co-precipitates with both Laves and δ phases, showing that the higher number of carbonitride precipitates in the reinforced sample is effective in absorbing Nb and Mo from the matrix.

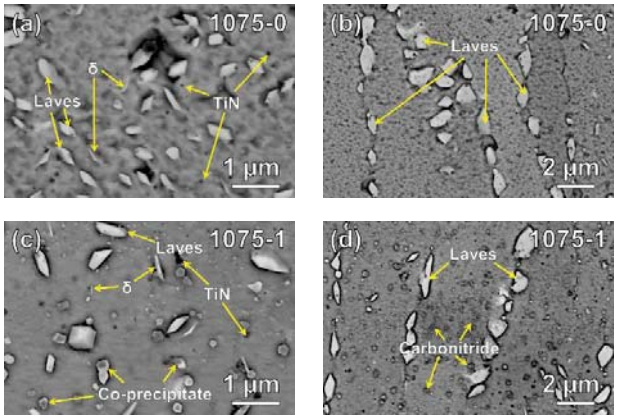

Fig. 2 SEM images comparing the microstructure between samples 1075-0 (a)(b) and 1075-1 (c)(d).

An interfacial layer (white color) is observed to form as shown in Fig. 3a. An intermediate layer (grey color) between the micron-TiC particles and the interfacial layer is also observed, indicating that there is a strong bonding between the micron-TiC particle and the interfacial layer. The observations suggest that the micron-TiC particles are favorable sites for Nb and Mo to diffuse towards. It is believed that the growth of the interfacial layer is based on the Ostwald ripening mechanism, which operates based on the transport of atoms in the microstructure and is related to the diffusion coefficient of the transported material [9].

The grains in sample 1275-0 (Fig. 3b) are observed to be larger than in sample 1275-1 (Fig. 3d). The grain refinement is due to the numerous precipitates at the grain boundaries and the homogeneously dispersed micron-TiC particles suppressing grain growth as a result of the Zener pinning effect [10]. The addition of micron-TiC particles reduces the segregation at the grain boundaries noticeably as shown in Fig. 3c and 3e. This is the result of micron-TiC particles absorbing solute elements and an increase in grain boundary length in sample 1275-1.

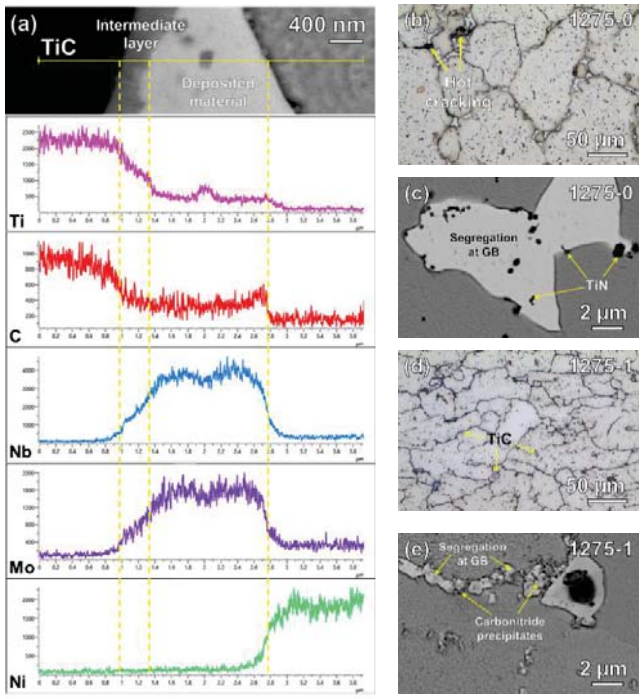

Fig. 3 Line scan EDX analysis showing the variation of chemical compositions (cps) between the micron-TiC particle, the interfacial layer, and the matrix (a). Optical micrographs of samples 1275-0 (b) and 1275-1 (d) after etching. Backscattered SEM images showing segregation at the grain boundary of samples 1275-0 (c) and 1275-1 (e).

2.3 Aged samples

Smaller grain size is observed in the reinforced sample after being heat treated as listed in Table 1. To understand the reasons behind the differences in the mechanical properties of the samples after aging treatment, all the samples are subjected to solutionizing treatment at 1275 ^{o}C before aging. This is because the diffusion of different alloying elements is significantly enhanced. As such, the movements of the alloying elements during heat treatment can be visualized.

Table 1 Grain sizes (μm) of printed samples under different conditions.

AP-0	AP-1	1075A-0	1075A-1	1275A-0	1275A-1
18.9 ± 1.9	16.9 ± 2.9	18.9 ± 4.4	13.4 ± 3.4	67.7 ± 20.7	29.1 ± 8.5

The distributions of the γ' and γ'' precipitates are different in the samples 1275A-0 and 1275A-1 as shown in Fig. 4. The γ' and γ'' precipitates are seen abundantly (71.0% of the total image area) near the grain boundaries in sample 1275A-0 (Fig. 4a). However, few

precipitates are seen far from the grain boundaries (Fig. 4b), which only occupied 52.0%. On the other hand, the distributions and the sizes of the precipitates in sample 1275A-1 are quite similar in both locations (Fig. 4c and d).

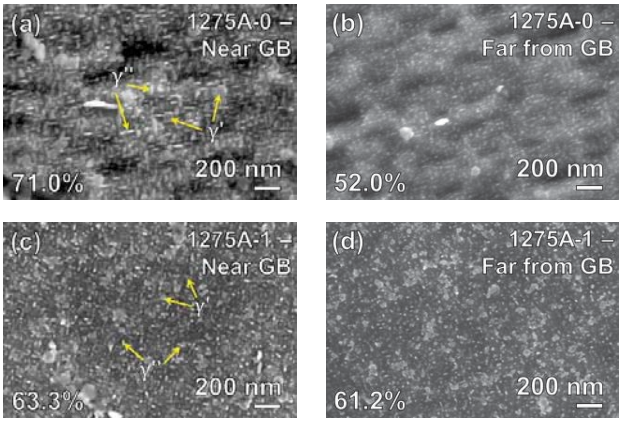

Fig. 4 SEM images showing the precipitates in sample 1275A-0 near grain boundary (a) and far from grain boundary (b), and in sample 1275A-1 near grain boundary (c) and far from grain boundary (d). GB: grain boundary.

This is due to the larger grain size and the segregation of Nb at the grain boundaries in sample 1275A-0, there is an Nb concentration gradient from the center of the grain to the edge of the grain as Nb diffuses towards the grain boundaries. Thus, this creates regions of low concentration of Nb at the center of the grains (red color) and regions of high concentration of Nb near the segregated materials at the grain boundaries (blue color) as shown in Fig. 5. As Nb is needed for the formation of both the γ' and γ'' precipitates, there will be more and bigger precipitates in the blue regions in sample 1275A-0. The absence of these factors in sample 1275A-1 resulted in a more homogeneous distribution of Nb.

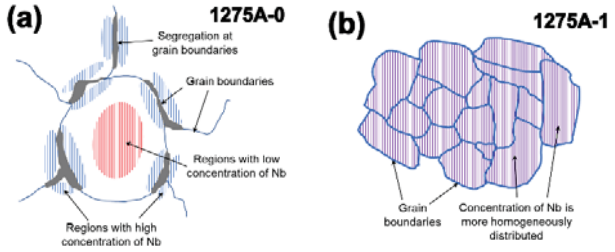

Fig. 5 Schematics showing the difference in the distribution of Nb in the microstructures after aging between samples 1275A-0 (a) and 1275A-1 (b).

3. Mechanical properties

Mechanical testing is carried out at the optimum heat treatment parameter settings. The strength of the TiC-reinforced sample is always higher than that of the non-reinforced sample under all conditions as shown in Fig. 6. In addition, the TiC-reinforced sample consistently has higher microhardness than the non-reinforced sample regardless of the stage of the heat treatment as listed in Table 2. The improvements in strength and microhardness of the reinforced sample are due to the following factors. Firstly, the higher number of carbonitride precipitates in the TiC-reinforced sample increases their Orowan strengthening contribution. Secondly, the grain refinement effect in the TiC-reinforced sample also plays a part in the higher strength and microhardness. Lastly, the lack of proper precipitation at the center of the grains and the coarsening of the γ' and γ'' precipitates near the grain boundaries affect the mechanical properties of the non-reinforced sample negatively.

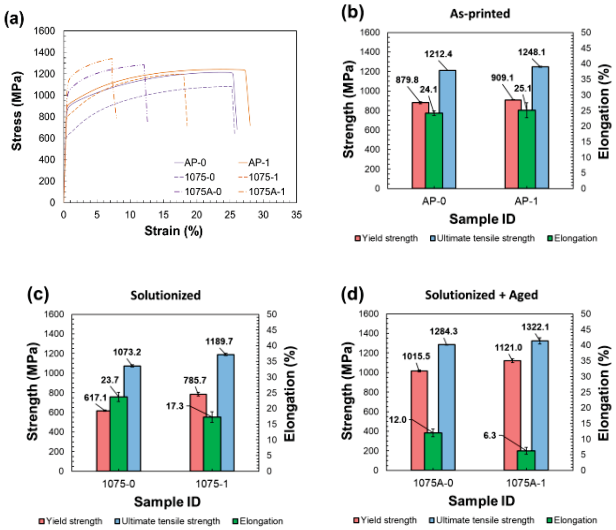

Fig. 6 Stress-strain curves (a) and tensile properties of as-printed (b), after solutionized (c), and after solutionized + aged (d) TiC reinforced samples in comparison with non-reinforced samples.

Table 2 Microhardness value (Hv) of printed samples under different conditions.

AP-0	AP-1	1075-0	1075-1	1075A-0	1075A-1
350.4 ± 4.8	388.8 ± 5.4	327.0 ± 11.7	402.2 ± 8.0	457.8 ± 7.0	502.2 ± 7.2

4. Conclusions

The addition of micron-TiC particles restricted grain growth during heat treatment. Solute materials are absorbed by the micron-TiC particles through Ostwald ripening mechanism instead of diffusing to the grain boundaries. This forms an interfacial layer between the particles and the IN718 matrix and reduces the segregation at the grain boundaries. Nano-sized carbonitride precipitates are formed due to the partial dissolution of micron-TiC particles and are still present after heat treatment. The diffusion of Nb towards the grain boundaries during aging creates a concentration gradient, affecting the amount and size of the γ' and γ'' precipitates in the aged sample. This mostly affects the non-reinforced IN718 sample due to it having large grains and highly segregated grain boundaries. The higher strength of the composite is achieved due to grain boundary strengthening, increased Orowan strengthening from a higher number of carbonitride precipitates, reduction of segregation at grain

boundaries, and the γ' and γ'' precipitates being distributed more homogeneously.

ACKNOWLEDGEMENT

The work is supported by the A*STAR Additive Manufacturing Centre (AMC) Initiative: Work Package I (High Temperature Materials Development for 3D Additive Manufacturing) with project No. 142 68 00088 and supported by the Nanyang Technological University. The authors would also like to thank Mr. Min Hao Goh for his assistance with the SEM analysis.

REFERENCES

[1] H. J. Wagner and A. M. Hall, *Physical metallurgy of Alloy 718*. The University of Michigan: Defense Metals Information Center, Battelle Memorial Institute, 1965.

[2] W. S. Miller and F. J. Humphreys, "Strengthening mechanisms in particulate metal matrix composites," *Scr. Metall. Mater.*, vol. 25, no. 1, pp. 33–38, Jan. 1991, doi: 10.1016/0956-716X(91)90349-6.

[3] D. Deng, J. Moverare, R. L. Peng, and H. Söderberg, "Microstructure and anisotropic mechanical properties of EBM manufactured Inconel 718 and effects of post heat treatments," *Mater. Sci. Eng. A*, vol. 693, no. December 2016, pp. 151–163, 2017, doi: 10.1016/j.msea.2017.03.085.

[4] Y. Wang and J. Shi, "Effect of post heat treatment on the microstructure and tensile properties of nano TiC particulate reinforced Inconel 718 by selective laser melting," *J. Manuf. Sci. Eng. Trans. ASME*, vol. 142, no. 5, pp. 1–12, 2020, doi: 10.1115/1.4046646.

[5] X. Yao, S. K. Moon, B. Y. Lee, and G. Bi, "Effects of heat treatment on microstructures and tensile properties of IN718/TiC nanocomposite fabricated by selective laser melting," *Int. J. Precis. Eng. Manuf.*, vol. 18, no. 12, pp. 1693–1701, 2017, doi: 10.1007/s12541-017-0197-y.

[6] Y. Wang, J. Shi, S. Lu, and Y. Wang, "Solution and aging treatments of Inconel 718/TIC nanocomposite from selective laser melting," *ASME 2016 11th Int. Manuf. Sci. Eng. Conf. MSEC 2016*, vol. 3, pp. 1–9, 2016, doi: 10.1115/MSEC20168684.

[7] C. Kumara, A. R. Balachandramurthi, S. Goel, F. Hanning, and J. Moverare, "Toward a better understanding of phase transformations in additive manufacturing of Alloy 718," *Materialia*, vol. 13, no. August, p. 100862, 2020, doi: 10.1016/j.mtla.2020.100862.

[8] D. Gu, H. Zhang, D. Dai, M. Xia, C. Hong, and R. Poprawe, "Laser additive manufacturing of nano-TiC reinforced Ni-based nanocomposites with tailored microstructure and performance," *Compos. Part B Eng.*, vol. 163, no. December 2018, pp. 585–597, 2019, doi: 10.1016/j.compositesb.2018.12.146.

[9] I. M. Lifshitz and V. V. Slyozov, "The kinetics of precipitation from supersaturated solid solutions," *J. Phys. Chem. Solids*, vol. 19, no. 1–2, pp. 35–50, 1961, doi: 10.1016/0022-3697(61)90054-3.

[10] G. S. Rohrer, "Introduction to grains, phases, and interfaces - an interpretation of microstructure," *Metall. Mater. Trans. A Phys. Metall. Mater. Sci.*, vol. 175, no. 5, pp. 15–51, 1948, doi: 10.1007/s11661-010-0215-5.